Journal of
Materials in Life Sciences

Vol. 4 No. 2 (2025)

Full Paper

In silico Evaluation of ssDNA Aptamer against 2GHV of SARS-CoV

Nur Hasya Abd Halim[a], Huszalina Hussin[a], Razauden Mohamed Zulkifli[a*]

[a] Department of Biosciences, Faculty of Science, Universiti Teknologi Malaysia, 81310, UTM Johor Bahru, Johor, Malaysia

Article history
Received
12 June 2025
Revised
26 October 2025
Accepted
28 October 2025
Published online
30 November 2025

*Corresponding author
razauden@fbb.utm.my

Abstract

SARS is an infectious disease that caused a global outbreak due to the novel coronavirus (SARS-CoV). This disease could cause severe symptoms in humans and even lead to fatality. The screening of SARS can be challenging, whether in terms of cost, time or energy. The goal of this study is to investigate the potential binding of the CoV-RBD-1C aptamer, which was retrieved from a previously reported journal. This aptamer targets 2GHV, the SARS-CoV spike protein receptor binding domain (RBD), obtained from the Protein Data Bank (PBD). Several bioinformatics tools, including Mfold, RNAComposer, and PyMOL, were used to design the predicted aptamer. The structures for both aptamer and target protein were minimized using GROMACS software, and the HDOCK web server was used as a docking tool. The optimization strategy for improving the aptamer's binding affinity was only conducted with the truncation method. The results indicated that the binding affinity between the optimized aptamer and the target protein is higher compared to the unrefined aptamer. The study also documented the incorporation of the chosen reporter, DAPI, into the designed ssDNA aptamer and then bound it against the target protein. The result showed that the binding affinity of RBC-APT01-DAPI-2GHV was significantly higher than that of RBC-APT-2GHV. The incorporation of ssDNA aptamer-reporter into the target protein suggests that the aptamer may be designed as an aptasensor in the future. This RBC-APT01-DAPI-2GHV also provides an opportunity for creating a new technique for the recognition of SARS-CoV and also helps in the diagnosis of the disease.

Keywords: aptamer, docking, in silico, molecular modelling, SARS-CoV

1.0 INTRODUCTION

Severe acute respiratory syndrome (SARS) is a contagious disease that first emerged in Guangdong Province of southern China, back in November 2002, before it spread to other countries resulting in a global outbreak [1]. The World Health Organization (WHO) reported that the disease was linked to a coronavirus, subsequently called SARS-associated coronavirus (SARS-CoV). It was believed that SARS-CoV spread from infected persons via close contact, as well as airborne and fomite routes [2]. When the infected person sneezes or coughs without covering their mouth, the respiratory droplet or aerosol from that action can be inhaled through the nose or mouth of someone nearby [3]. The symptoms that commonly appear in an infected person include a high fever exceeding 38.0°C, headache, abdominal pain, dry cough, and certain people might also experience diarrhea [4]. Over time, some individuals may develop more severe symptoms like pneumonia, which can lead to acute respiratory distress or even be fatal. Scientists have been making an effort to search for a treatment for SARS, employing various methods, including aptamers.

Aptamers are short single-stranded oligonucleotides that bind to specific targets with high affinity and specificity and are known for their versatility. Aptamers are produced through a process called systematic evolution of ligands by exponential enrichment (SELEX). On top of that, there has been an alternative strategy to SELEX, which is applying a computational method. In 2015, a study by Zhou et al. in testing the in silico SELEX was proven to have high potential as a method in designing and optimizing aptamer structures [5, 6]. Aptamers have become widely used by researchers due to their numerous advantages. They are highly stable, maintaining their structure at high temperatures, and can be synthesized in large quantities with remarkable accuracy. Besides that, they have low immunogenicity, which makes the human immune system unable to recognize them as foreign agents, giving a high possibility to successfully enter the body. Last but not least, aptamers exhibit a high potential to bind to various targets, including ligands that are known to be quite challenging for antibodies to recognize [7]. Using a computational approach, this study aims to predict and investigate the interaction of the binding of the designed aptamer to the target protein.

The crystal structure of the SARS-CoV spike receptor-binding domain has been discovered and deposited in the Protein Data Bank (PDB) (PDB ID: 2GHV) [8]. The spike glycoprotein facilitates viral entry into the host cell by binding its receptor binding domain (RBD) to the human cell receptor angiotensin-converting enzyme 2 (ACE2) [9]. In a previous study, because both SARS-CoV and SARS-CoV-2 RBDs recognize the same ACE2 receptor, a previously developed aptamer targeting the SARS-CoV-2 spike RBD may also exhibit binding affinity for the SARS-CoV RBD. However, this potential cross-reactivity has not been systematically assessed. The objective of this study is to investigate the binding capability of a reported SARS-CoV-2 RBD-binding aptamer against the SARS-CoV RBD.

2.0 MATERIALS AND METHODS

The workflow in this study involved three major stages, which are structure minimization, molecular docking, and structure optimization through truncation. Firstly, energy minimization was performed to refine the 3D structures of both the target protein and the aptamer, thereby ensuring structural stability prior to docking. Subsequently, molecular docking simulations were conducted to predict the binding affinity and interaction analysis of the complex structure. Followed by docking analysis, structural optimization was achieved by truncating the non-essential nucleotide sequence of the aptamer in order to improve stability, reduce steric hindrance, and enhance binding specificity. This systematic approach provided a reliable framework to evaluate and refine the aptamer-protein interaction.

2.1 The Selection Sequences of ssDNA Aptamer

The ssDNA sequences of the aptamer used in this study were derived from the research group [10] that has successfully designed the sequences CoV2-RBD-1C and CoV2-RBD-4C. These aptamers were developed through twelve rounds of SELEX procedure targeting the RBD of SARS-CoV-2 spike glycoprotein. For this study, CoV2-RBD-1C was selected to bind to 2GHV, focusing on the potential of this aptamer to attach to the SARS-CoV protein.

2.2 The Generation of the 3D Structure of ssDNA Aptamer

The development of 3D structure began with examining the primary sequence of selected aptamers, using the Mfold web server for secondary folding structure prediction and hybridization. The obtained secondary structure was further submitted to RNAComposer, an automated RNA 3D modelling server, to generate the corresponding 3D RNA model [1]. Following that, the 3D RNA model was converted into a 3D ssDNA model, manually by using PyMOL. The conversion involved two major steps: modification of uracil to thymine and modification of the ribose sugar backbone to deoxyribose. The obtained predicted aptamer structure was then named RBC-APT.

2.3 The Refinement of 2GHV and RBC-APT Model

Energy minimization was performed on both the structure of RBC-APT and 2GHV, using GROMACS with the CHARMM27 force field. The success of energy minimization was determined by analyzing the em.edr file, and after 1000 steps of steepest descent minimization, the average potential energy (Epot) was plotted using Xmgrace [11]. The energy-minimized structure was then implemented for molecular docking studies.

2.4 Molecular Docking of RBC-APT and 2GHV

RBC-APT-2GHV docking was conducted using HDOCK [12]and ZDOCK [13]. The RBC-APT was designated as the ligand and 2GHV as the receptor. The objective of the docking procedure was to identify which base of the aptamer interacted with 2GHV. RBC-APT-2GHV complex with the lowest docking score, was chosen based on the ranking system provided by these automated docking tools.

2.5 Optimization of RBC-APT by Truncation

Truncation was performed where the non-essential nucleotides were removed to enhance the properties of the aptamer [14]. After the 3D structure of truncated aptamer (RBC-APT01) was generated with similar steps, docking was conducted on RBC-APT01 against 2GHV using HDOCK. The model which exhibits the lowest docking score was selected for further analysis as the complex of interest.

2.6 Molecular Docking of RBC-APT01-2GHV Complex and Reporter Molecule

Following the docking analysis results, the next step involves exploring the possibility of incorporating a reporter into the RBC-APT01. In this study, a 4', 6-diamidino-2-phenylindole (DAPI) reporter was chosen (Figure 1). DAPI was applied in previous research for a biosensor application [14, 15]. It is prudent to select a reporter that has been demonstrated to successfully bind to an aptamer or any target. DAPI was retrieved from the PubChem database. Subsequently, RBD-APT01-DAPI docking was performed using HDOCK. Following this, docking was conducted between RBC-APT01-DAPI and 2GHV. Then, the model with the highest docking score is selected for further analysis. The intermolecular interaction in the complex, RBC-APT-2GHV, RBC-APT01-2GHV, RBC-APT01-DAPI and RBC-APT01-DAPI-2GHV, was visualized and studied using PyMOL and Discovery Studio Visualizer (DSV).

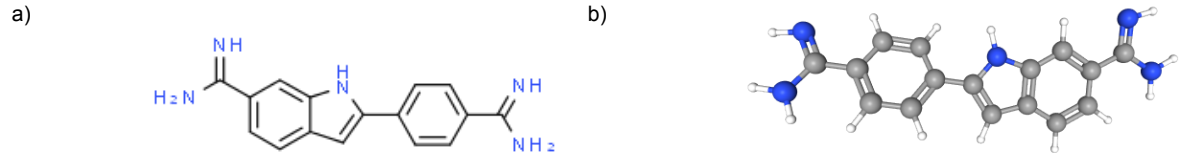

Figure 1: a) Secondary structure of DAPI, b) Tertiary structure of DAPI [17]

3.0 RESULTS AND DISCUSSION

3.1 Subtopic Modelling 3D Structural Prediction of Aptamer and Refinement of RBC-APT and 2GHV

The essential element of this study is to investigate the potential cross-reactivity of an aptamer originally developed against the SARS-CoV-2 RBD toward the SARS-CoV RBD. Indicating such binding capability would not only provide insights into the structural similarities between these two proteins but also widen the applicability of the existing aptamer-based recognition elements.

Following the methodology outlined in the Experimental Design section, the predicted 3D structure was successfully identified. RBC-APT consists of three sets of conformations at Stem 1 (1-6, 25-30), Stem II (10-11, 21-22) and Stem III (31-35, 46-50) featuring an internal loop and two hairpin loops (Figure 2(a)). The structure was then followed by an automatically generated 3D structure using the RNAComposer webserver. Subsequently, both 3D ssDNA RBC-APT and 2GHV were refined by conducting energy minimization (Figure 2(b)(c)) using GROMACS as a pre-docking step.

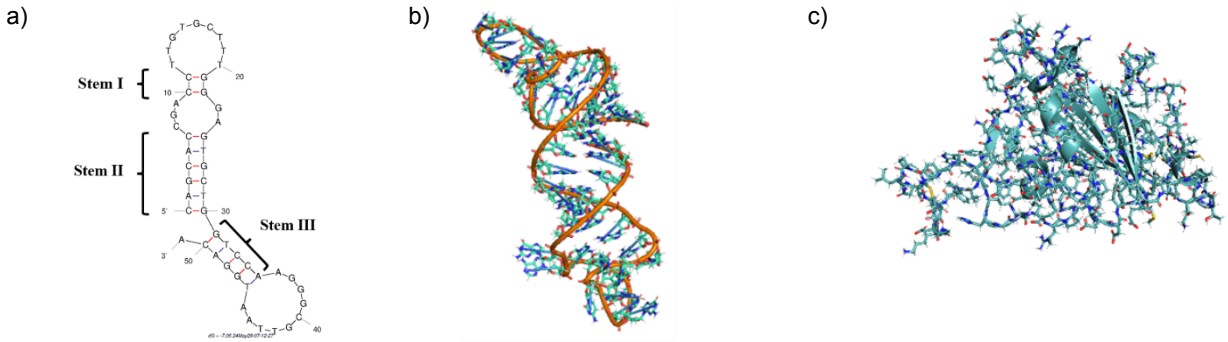

Figure 2: a) The 2D structure prediction of the aptamer and the refined structure [10] of b) RBC-APT and c) 2GHV [8]

3.2 Molecular Docking Between 2GHV and Cov2-RBD-1C ssDNA Aptamer

It is inarguable that different servers will provide various binding sites. Therefore, molecular docking simulation was done using two suitable docking tool web servers: HDOCK and ZDOCK. The best docking pose of RBD-APT in HDOCK score was -285.41. The docking result with an LGscore of 4.048 and a MaxSub of 0.174 further demonstrated the quality of the docking structures data. Both of these scores are in an acceptable range. In ZDOCK, we correspondingly picked the model with the highest ZDOCK score. The comparison model of HDOCK and ZDOCK is shown in Figure 3.

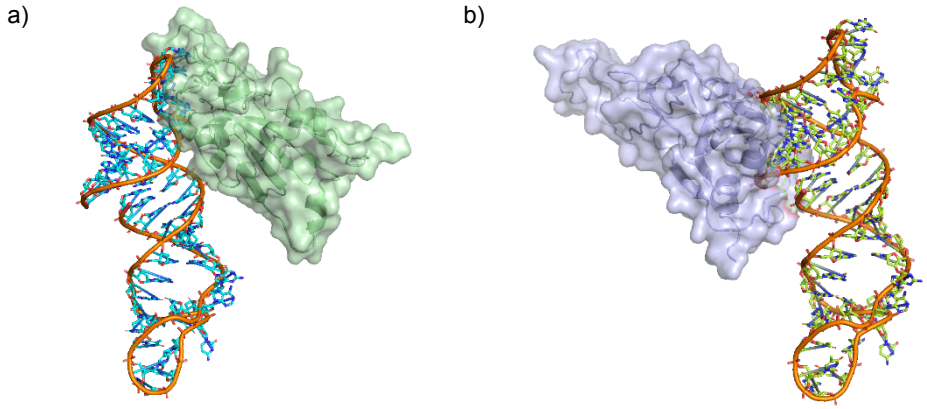

Figure 3: a) RBC-APT and 2GHV complex from HDOCK, b) RBC-APT and 2GHV complex from ZDOCK

In order to explore the potential of RBD-APT as a ligand in binding against SARS-CoV, analysis for the complex docking structures from both HDOCK and ZDOCK using DSV software was conducted. In HDOCK (Table 1), the interactions near the 3' terminal of RBD-APT showed that the binding interface included DG38, DT29, DT43, DT42, DT43 and DG41, which formed hydrogen bonds with TYR436, THR402, TYR408, TYR442, ARG444 and LYS390, respectively. The formation of hydrogen bonds between the aptamer and protein is crucial for stabilizing the protein at the aptamer binding site. These bonds are categorized by donor-acceptor distances: 2.2-2.5 Å as "strong, mostly covalent", 2.5-3.2 Å as "moderate", and 3.2-4.0 Å as "weak" [18]. On top of that, the formation of a salt bridge between DT29 and LYS447 was observed. This interaction falls within the hydrogen bonds category, but with the combination of hydrogen bond and ionic bonding, making it equally important for protein stability [19]. Moreover, 3 attractive charge interactions were formed between DC28, DT46 and DG47 with ARG395 while all within the maximal charge-charge distance of 5.6 Å. These electrostatic interactions significantly contribute to the aptamer's high affinity and specificity in binding to the protein. Figure 4 shows the interaction between the RBC-APT structure and the 2GHV structure from HDOCK output.

Table 1: Interaction information of RBC-APT-2GHV using HDOCK

Interacting base	Residue	Distance (Å)	Types of interaction
DG38:O3'	TYR436:OH	2.49428	Conventional Hydrogen Bond
DT29:O2P	THR402:OG1	2.4949	Conventional Hydrogen Bond
DT43:O2	TYR408:OH	2.7195	Conventional Hydrogen Bond
DT42:O4	TYR442:OH	2.9182	Conventional Hydrogen Bond
DT43:O2	ARG444:N	3.14117	Conventional Hydrogen Bond
DG41:O6	LYS390:NZ	3.19311	Conventional Hydrogen Bond
DT29:O1P	LYS447:NZ	3.64514	Salt Bridge
DC28:O2P	ARG395:NH2	4.39935	Attractive Charge
DT46:O1P	ARG395:NH1	4.52605	Attractive Charge
DG47:O2P	ARG395:NH2	5.51874	Attractive Charge

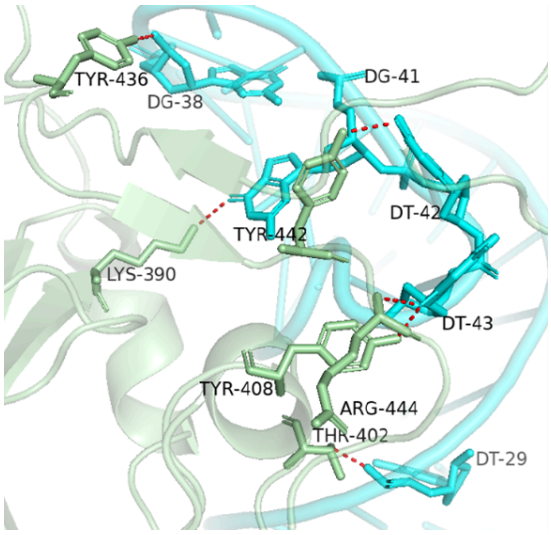

Figure 4: The structure of RBC-APT (cyan) bound to 2GHV (pale green) that formed hydrogen bonds from HDOCK docking

Comparatively, the binding interaction from ZDOCK formed hydrogen bonds between DA51, DA49, DA2 of RBC-APT and TYR356, CYS378, SER353 of 2GHV, respectively (Table 2). Nonetheless, the interaction formed a Pi-Pi T-shaped, including DA51-PHE360 and DA49-PHE364. Pi-Pi T-shaped is one of the hydrophobic interactions. It is a direct attractive non-covalent interaction between aromatic rings through a T-shaped and this interaction also majorly contributes to the stability of the complex structure [16, 18]. DC34 also formed 1 attractive charge interaction with LYS365 with a distance of 4.8 Å. Figure 5 shows the interaction between the RBC-APT structure and the 2GHV structure from the ZDOCK output.

Table 2: Interaction information of RBC-APT-2GHV using ZDOCK

Interacting base	Residue	Distance (Å)	Types of interaction
DA51:O3'	TYR356:N	2.49764	Conventional Hydrogen Bond
DA49:O1P	CYS378:SG	3.01509	Conventional Hydrogen Bond
DA2:O1P	SER353:OG	3.28565	Conventional Hydrogen Bond
DA51	PHE360	3.94555	Pi-Pi T-shaped
DA49	PHE364	4.24853	Pi-Pi T-shaped
DC34:O1P	LYS365:NZ	4.83861	Attractive Charge

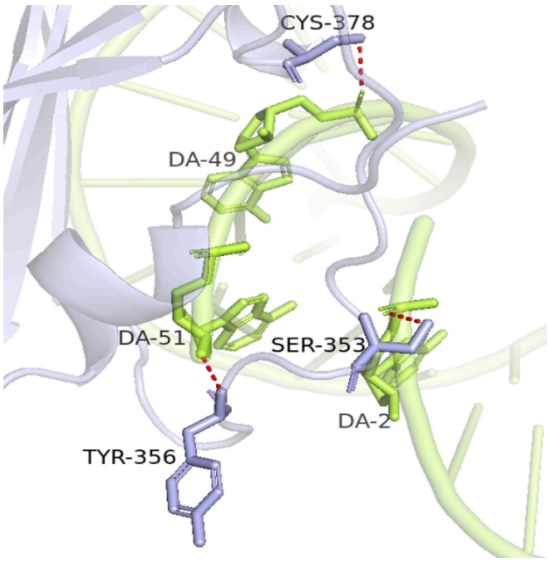

Figure 5: The structure of RBC-APT (lemon green) bound to 2GHV (slate) that formed hydrogen bonds from ZDOCK docking

The binding interaction of RBC-APT-2GHV, both from HDOCK and ZDOCK, was compared with the binding interaction of CoV2-RBD-1C-SARS-CoV-2 S protein complex by Song's group [10] as detailed in Table 3. Most interacting

bases of the aptamer identified by HDOCK were consistent with those reported, while ZDOCK showed no similarities and even fewer interactions compared to the reported aptamer. Thus, HDOCK webserver was chosen as it produces better results than ZDOCK webserver. This clearly demonstrates that the aptamer can potentially recognize SARS-CoV spike protein RBD, despite its differences from SARS-CoV-2 spike protein RBD. Apart from that, the identified binding site of the aptamer, particularly the essential nucleotides, was highlighted as a foundation for optimizing the aptamer.

Table 3: Comparison in binding interaction between RBC-APT-2GHV complex from HDOCK, ZDOCK and reported CoV2-RBD-1C-SARS-CoV-2 S protein complex by Yanling Song'group.

RBC-APT-2GHV complex from HDOCK		RBC-APT-2GHV complex from ZDOCK		CoV2-RBD-1C-SARS-CoV-2 S protein complex	
Interacting base	**Residue**	**Interacting base**	**Residue**	**Interacting base**	**Residue**
DG38:O3'	TYR436:OH	DA51:O3'	TYR356:N	T42[c]	THR500
DT29:O2P[a]	THR402:OG1	DA49:O1P	CYS378:SG	T43[b]	GLN506
DT43:O2[b]	TYR408:OH	DA2:O1P	SER353:OG	T43[b]	ASN437
DT42:O4[c]	TYR442:OH	DA51	PHE360	G30	SER375
DT43:O2[b]	ARG444:N	DA49	PHE364	T29[a]	PHE374
DG41:O6	LYS390:NZ	DC34:O1P	LYS365:NZ	C28[d]	ALA372
DT29:O1P[a]	LYS447:NZ			G3	ALA372
DC28:O2P[d]	ARG395:NH2			C4	ASN370
DT46:O1P	ARG395:NH1				
DG47:O2P	ARG395:NH2				

Notes: The cell that has a similar lowercase alphabet is indicated to have a similar nucleotide base.

3.3 Optimization of the ssDNA Aptamer

In order to optimize the aptamer structure, truncation was conducted to improve its stability (Gao et al., 2016). The nucleotide structure that was not involved in binding with 2GHV (RBC-APT01: 5'-GGTCCAAGGGCGTTAATGGACA-3') was removed. Then, its capability in binding against 2GHV was evaluated. Figure 6 depicts the docking structure of RBC-APT01-2GHV. The docking score of the selected model is -287.52, while the LGscore and MaxSub value are the same as the RBC-APT-2GHV complex, indicating the preservation of the docking structure's quality. The docking score between RBC-APT-2GHV and RBC-APT01-2GHV was compared in Table 4. The results demonstrated that the RBC-APT01-2GHV complex had a significantly higher docking score than the RBC-APT-2GHV complex. This suggests that nonessential nucleotides may restrict the binding properties of the aptamer; therefore by removing them reduces steric interference [9, 13].

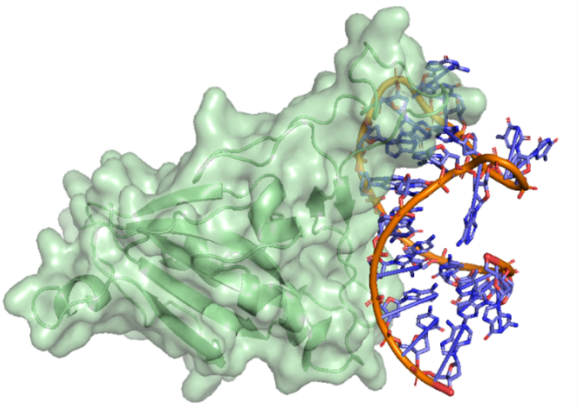

Figure 6: The structure of RBC-APT01 (slate) and 2GHV (pale green) after docking

Table 4: Comparison of the summary result from HDOCK between RBC-APT-2GHV complex and RBC-APT01-2GHV complex

	RBC-APT-2GHV complex	RBC-APT01-2GHV complex
Docking score	-285.41	-287.52
LGscore	4.048	4.048
MaxSub	0.174	0.174

The binding interaction of the RBC-APT01-2GHV complex showed fewer interactions compared to the RBC-APT-2GHV complex (Table 5). Only 2 moderate-strength hydrogen bonds were formed between DG18 and DC5 with ASN479 and TYR436, respectively. Additionally, attraction charge interaction occurred between DG8 and LYS439, and between DA20 and LYS390, with distances of 4.0Å and 4.7Å, respectively. These findings prove that the improvement in binding affinity resulted not from intermolecular interactions alone, but from an effective optimization strategy.

Table 5: The interaction analysis of RBC-APT01-2GHV complex

Interacting base	Residue	Distance (Å)	Type of interaction
DG18:N3	ASN479:ND2	2.98041	Conventional Hydrogen Bond
DC5: O2	TYR436:OH	3.382	Conventional Hydrogen Bond
DG8:O1P	LYS439:NZ	4.05197	Attractive Charge
DA20:O1P	LYS390:NZ	4.75723	Attractive Charge

3.4 Integration of DAPI Into the Truncated ssDNA Aptamer

The aim of this step is to introduce a fluorochrome that would emit a fluorescence signal upon binding to the target, facilitating observation in future experiments. DAPI was chosen as the reporter. DAPI is recognized for its role as a fluorochrome and is capable of enhancing significant fluorescence signals [21]. In a previous experiment conducted by Zhu's group, DAPI, a minor groove binding dye, was utilized in label-free aptamer-based sensors to detect L-argininamide. This method was noted for its speed, simplicity and cost-effectiveness. Zhu's group found the increasing binding affinity of DAPI to the aptamer, resulting in enhanced fluorescence upon binding to the target [21]. Therefore, DAPI shows promise for incorporation into aptamers targeting specific proteins.

Docking was first conducted between DAPI and RBC-APT01 using HDOCK. Next, the complex was docked with the 2GHV structure (Figure 7). Following that, RBC-APT01-DAPI-2GHV complex achieved a docking score of -289.12, maintaining the quality of the initial docking structure, as there were no significant changes in the complex conformation post-binding. Table 6 presents a comparison of the docking score between the RBC-APT01-2GHV complex and the RBC-APT01-DAPI-2GHV complex.

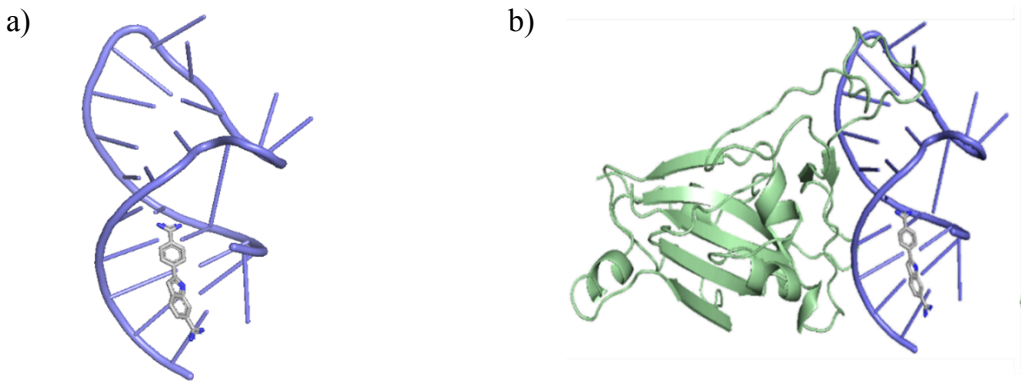

Figure 7: The model of RBC-APT01 with DAPI reporter and (B) RBC-APT01-DAPI-2GHV complex

Table 6: Comparison output between RBC-APT01-2GHV complex and RBC-APT01-DAPI-2GHV complex

	RBC-APT01-2GHV complex	RBC-APT01-DAPI-2GHV complex
Docking score	-287.52	-289.12
LGscore	4.048	4.048
MaxSub	0.174	0.174

The RBC-APT01-DAPI-2GHV complex indicates a lower docking score than the RBC-APT01-2GHV complex. This suggests that the aptamer retained its ability to recognize the target even in the presence of DAPI, simultaneously increasing its binding affinity. Another analysis was performed using DSV, with the results detailed in Table 7. The RBC-APT01-DAPI-2GHV complex exhibits more intermolecular interactions and shorter donor-acceptor and charge-charge distances (Å), which likely contributed to improving binding affinity. The detailed structure with interactions was shown in Figure 8.

Table 7: Interaction analysis of RBC-APT01-DAPI-2GHV complex

Interacting base	Residue	Distance (Å)	Type of interaction
DG18:N3	ASN479:ND2	2.52633	Conventional hydrogen bond
DG19:N3	TYR436:OH	3.12091	Conventional hydrogen bond
DA7:O3'	LYS439:NZ	3.30291	Conventional hydrogen bond
DA20:O1P	LYS390:NZ	4.10331	Attractive charge
DG8:O1P	LYS439:NZ	4.18088	Attractive charge

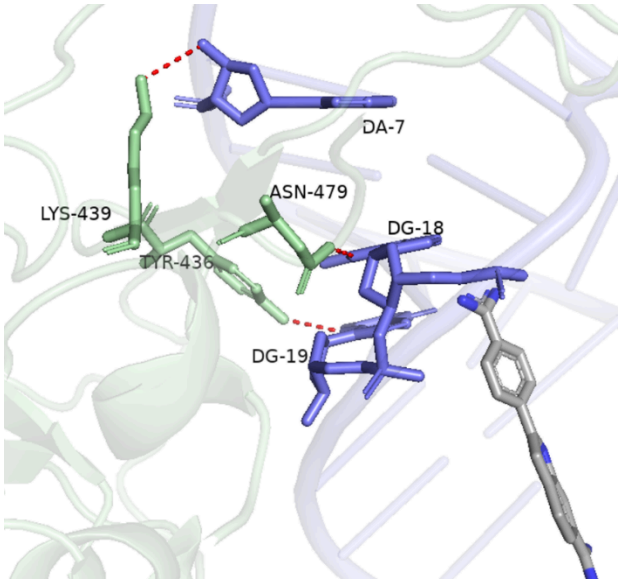

Figure 8: The structure with interaction between RBC-APT01-DAPI and 2GHV

Nevertheless, the reporter successfully bound to both RBC-APT01 and 2GHV, and managed to enhance the binding affinity, suggesting its potential utility for recognition expressed on SARS-CoV. This shows that the reporter could be effectively employed in applications aimed at detecting SARS-CoV, demonstrating its potential utility in various experimental and diagnostic contexts.

4.0 CONCLUSION

This *in silico* study demonstrates that RBC-APT, the reported SARS-CoV-2 RBD-binding aptamer, has potential against the SARS-CoV RBD. The optimized RBC-APT01 using the truncation strategy leads to enhanced binding affinity and reduced costs for future aptamer synthesis. Lastly, DAPI shows a potential for incorporation into RBC-APT01, enhancing its binding with 2GHV and suggesting potential utility in recognizing SARS-CoV in future applications. Nonetheless, further research involving molecular dynamics simulation is necessary for gaining deeper insights into the patterns of interaction between the aptamer and target protein.

Acknowledgment

The authors would like to thank the Department of Bioscience, Faculty of Science, Universiti Teknologi Malaysia, for supporting this project and gratefully acknowledge the financial support provided by *Geran Penyelidik Baharu* (PY/2024/02290) from Universiti Teknologi Malaysia.

References

1. Biesiada, M., Pachulska-Wieczorek, K., Adamiak, R. W., & Purzycka, K. J. (2016). RNAComposer and RNA 3D structure prediction for nanotechnology. *Methods, 103*, 120–127.
2. Xiao, S., Li, Y., Wai Wong, T., & Hui, D. S. C. (2017). Role of fomites in SARS transmission during the largest hospital outbreak in Hong Kong. *PLoS One, 12*(7).
3. Shereen, M. A., Khan, S., Kazmi, A., Bashir, N., & Siddique, R. (2020). COVID-19 infection: Origin, transmission, and characteristics of human coronaviruses. *Journal of Advanced Research, 24*, 91–98.
4. Stadler, K., et al. (2003). SARS — Beginning to understand a new virus. *Nature Reviews Microbiology, 1*(3), 209–218.
5. Zhou, Q., Xia, X., Luo, Z., Liang, H., & Shakhnovich, E. (2015). Searching the sequence space for potent aptamers using SELEX in silico. *Journal of Chemical Theory and Computation, 11*(12), 5939–5946.
6. Chen, L., Zhang, B., Wu, Z., Liu, G., Li, W., & Tang, Y. (2023). In silico discovery of aptamers with an enhanced library design strategy. *Computational and Structural Biotechnology Journal, 21*, 1005–1013.
7. Song, K. M., Lee, S., & Ban, C. (2012). Aptamers and their biological applications. *Sensors, 12*(1), 612–631.
8. RCSB Protein Data Bank. (2025, August 18). *2GHV: Crystal structure of SARS spike protein receptor-binding domain.* Retrieved from https://www.rcsb.org/structure/2GHV
9. Cleri, F., Lensink, M. F., & Blossey, R. (2021). DNA aptamers block the receptor-binding domain at the spike protein of SARS-CoV-2. *Frontiers in Molecular Biosciences, 8*, 713003.
10. Song, Y., et al. (2020). Discovery of aptamers targeting the receptor-binding domain of the SARS-CoV-2 spike glycoprotein. *Analytical Chemistry, 92*(14), 9895–9900.
11. Singh, S., Sablok, G., Farmer, R., Singh, A. K., Gautam, B., & Kumar, S. (2013). Molecular dynamic simulation and inhibitor prediction of cysteine synthase structured model as a potential drug target for trichomoniasis. *BioMed Research International, 2013*, 390920.
12. Yan, Y., Zhang, D., Zhou, P., Li, B., & Huang, S. Y. (2017). HDOCK: A web server for protein–protein and protein–DNA/RNA docking based on a hybrid strategy. *Nucleic Acids Research, 45*(W1), W365–W373.
13. Pierce, B. G., Wiehe, K., Hwang, H., Kim, B. H., Vreven, T., & Weng, Z. (2014). ZDOCK server: Interactive docking prediction of protein–protein complexes and symmetric multimers. *Bioinformatics, 30*(12), 1771–1773.
14. Gao, S., Zheng, X., Jiao, B., & Wang, L. (2016). Post-SELEX optimization of aptamers. *Analytical and Bioanalytical Chemistry, 408*(20), 4567–4574.
15. Elskens, J. P., Elskens, J. M., & Madder, A. (2020). Chemical modification of aptamers for increased binding affinity in diagnostic applications: Current status and future prospects. *International Journal of Molecular Sciences, 21*(12), 4522.
16. Wang, R. E., Zhang, Y., Cai, J., Cai, W., & Gao, T. (2011). Aptamer-based fluorescent biosensors. *Current Medicinal Chemistry, 18*(27), 4175–4184.
17. PubChem. (2025, August 18). *4',6-Diamidino-2-phenylindole | C16H15N5 | CID 2954.* Retrieved from https://pubchem.ncbi.nlm.nih.gov/compound/2954
18. Zulkeflee Sabri, M., Abdul Hamid, A. A., Sayed Hitam, S. M., & Abdul Rahim, M. Z. (2020). In-silico study of single-strand DNA aptamers against cortisol as a potential biomarker receptor in therapeutics and diagnostics. *Materials Today: Proceedings, 31*(Suppl 1), A90–A97.
19. Takano, K., Tsuchimori, K., Yamagata, Y., & Yutani, K. (2000). Contribution of salt bridges near the surface of a protein to the conformational stability. *Biochemistry, 39*(40), 12375–12381.
20. Zhao, Y., et al. (2015). Conformational preferences of π–π stacking between ligand and protein: Analysis derived from crystal structure data. *Interdisciplinary Sciences: Computational Life Sciences, 7*(3), 211–220.
21. Zhu, Z., Yang, C., Zhou, X., & Qin, J. (2011). Label-free aptamer-based sensors for L-argininamide by using nucleic acid minor groove binding dyes. *Chemical Communications, 47*(11), 3192–3194.